Received: 31 March 2018 | Revised: 3 August 2018 | Accepted: 2 September 2018

DOI: 10.4218/etrij.2018-0163

ORIGINAL ARTICLE

WILEY ETRI Journal

77-GHz mmWave antenna array on liquid crystal polymer for automotive radar and RF front-end module

Sangkil Kim[1] | **Amin Rida**[2] | **Vasileios Lakafosis**[2] | **Symeon Nikolaou**[3] | **Manos M. Tentzeris**[2]

[1]Department of Electronics Engineering, Pusan National University, Busan, Rep. of Korea.

[2]School of Electrical and Computer Engineering, Georgia Institute of Technology, Atlanta, GA, USA.

[3]Department of Electrical Engineering, Frederick University, Nicosia, Cyprus.

Correspondence
Sangkil Kim, Department of Electronics Engineering, Pusan National University, Busan, Rep. of Korea.
Email: ksangkil3@pusan.ac.kr

Funding information
Pusan National University

This paper introduces a low-cost, high-performance mmWave antenna array module at 77 GHz. Conventional waveguide transitions have been replaced by 3D CPW-microstrip transitions which are much simpler to realize. They are compatible with low-cost substrate fabrication processes, allowing easy integration of ICs in 3D multi-chip modules. An antenna array is designed and implemented using multilayer coupled-fed patch antenna technology. The proposed 16 × 16 array antenna has a fractional bandwidth of 8.4% (6.5 GHz) and a 23.6-dBi realized gain at 77 GHz.

KEYWORDS
3D transition, automotive radar module, broadband transition, mmWave antenna array, proximity-coupled patch antenna

1 | INTRODUCTION

According to a study by the World Health Organization, road traffic accidents are expected to increase from the 9th to 5th cause of death by 2030 [1]. This pushes for technological advancements in sensing and detection, which are a critical part of contemporary automotive technology (ie, self-driving autonomous cars). There are several features that can be integrated into vehicles for safer driving: adaptive cruise control, collision notification, avoidance, blind spot detection, park mate, back-up aid, lane departure warning, lane keeping, traffic sign recognition, and night vision. mmWave radar was once considered inappropriate technology for automotive applications because there were no practical means of generation, reception, channelization, and transmission of electromagnetic (EM) waves in the mmWave range. However, recent developments based on the mmWave theory and experimentation have provided new opportunities for communication and radar applications in various fields. The mmWave band offers many advantages compared to low-GHz frequency bands. It has a broad bandwidth, high communication security, small antenna dimensions, high-speed data transmission, and compatibility with Si technology [2,3]. Polished metallic structures have advantages such as low path loss, robust mechanical support, and high isolation from external noise. However, conventional metallic waveguide-based antennas and radio frequency (RF) module architectures for packaging, support, and interconnection have enormous costs and high volumes [4,5].

mmWave technology for short-range broadband radar and other applications is low-cost and has good performance. The ultimate goal of this study is to realize a low-cost, high-performance mmWave module that can be applied to automotive radar. In this work, a broadband 3D transition and a patch antenna array on a low-cost flexible liquid crystal polymer (LCP) substrate for

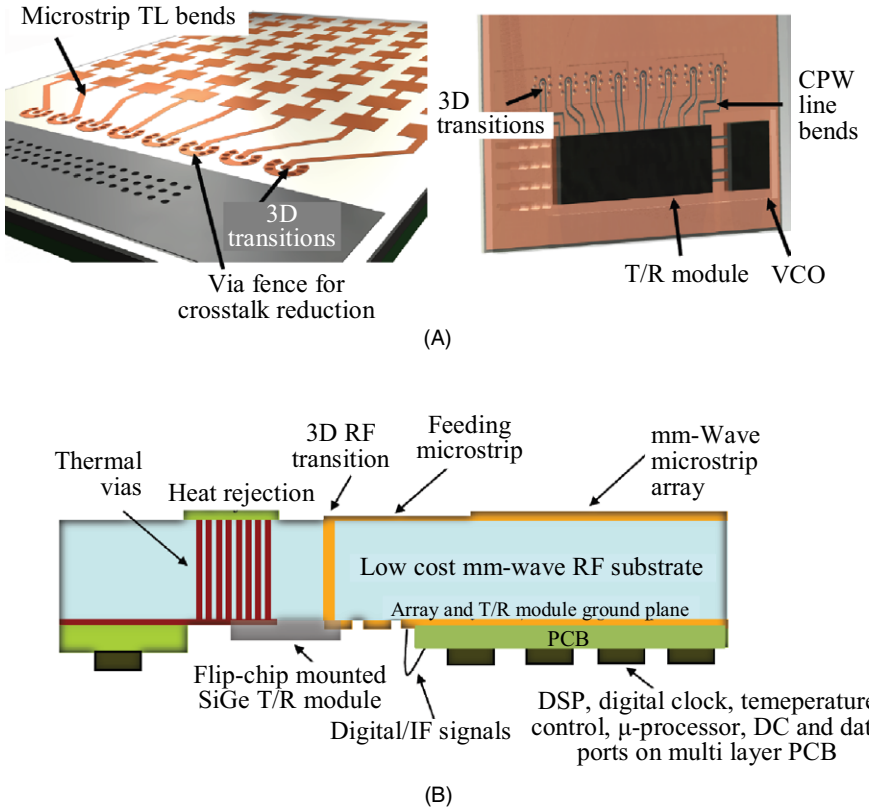

FIGURE 1 A, Front and back side view of proposed architecture for 3D-integrated mmWave radar front-end, and B, cross-section of multilayer low-cost RF mmWave front-end module based on FCBGA technology

mmWave applications are introduced as the first step toward this goal. The novelty of this paper is the presentation of the RF mmWave front-end module that replaces the waveguide structures with wideband coplanar-waveguide-(CPW)-based 3D RF transition while considering materials, packaging, integration, and antenna design. As shown in Figure 1, the proposed antenna array module has been designed based on flip chip ball grid array technology which is a key technology enabling compact RF front-end modules with high system integrity. Figure 1A shows a CPW line bending for system miniaturization and interconnection between integrated circuits (ICs) and the antenna array. Figure 1B shows the cross-section of the proposed module with a heat sink (through thermal vias), DSP, and digital blocks. A planar patch type antenna was designed as proof-of-concept since the automotive radar needs a broadside radiation pattern with a high antenna gain. The ground plane under the patch antennas efficiently isolates the analog/digital circuits from the radiation system (ie, antennas and their feeding networks) as shown in Figure 1B. The proposed antenna array for the mmWave module is an off-chip antenna architecture that exhibits better antenna performance (ie, radiation efficiency, heat sink, and gain); however, it requires a much larger area than the on-chip antenna. The on-chip antenna is able to reduce the module size dramatically, but the antenna suffers from low radiation efficiency owing to the silicon substrate which is a high-loss and thin material [6]. Waveguide aperture, patch, slot, Yagi-Uda, and Vivaldi antenna types are widely utilized in sub-THz (>100 GHz) on-chip antenna applications.

2 | INTERCONNECTIONS FOR MMWAVE RF FRONT-END

In this section, a development method for easy-to-fabricate low-cost wideband 3D transitions on flexible organic LCP is introduced for mmWave applications such as broadband high-speed wireless LAN, automotive radar, and imaging systems [7]. LCP has recently received great attention as a potential high-performance microwave medium with excellent dual functionality (substrate and packaging) owing to its excellent electrical, mechanical, and hermeticity properties. The reported dielectric constant (εr) and the loss tangent (tan δ) values of LCP are approximately 3.0 and 0.0035 at 77 GHz, respectively [8]. The substrate thickness was 100 μm and a full-wave 3D finite element method software tool (Ansys HFSS) was used in this work.

The recently reported micromachined 3D RF signal line transition on a Si substrate features good performance up to 50 GHz; however, it requires an expensive fabrication process as a result of the necessary formation of cavities [9]. Another reported broadband vertical transition has an

operation frequency range from DC to 60 GHz with a four-layer metal lamination [10]. Other reported research efforts are bulky and limited in bandwidth because of their waveguide-based structures [11, 12].

In this section, two simple wideband 3D transitions are presented. The CPW-CPW-MSTRIP and CPW-CPW transitions are printed on LCP. All dimensions of the designed structures were chosen based on existing design rules, including the use of mechanical drilling for via holes.

2.1 | Coplanar waveguide to microstrip line transition

The proposed design is shown in Figure 2A with all of the detailed dimensions. It achieved good wideband RF performance by utilizing a tapered ground plane and placing ground vias at appropriate locations to suppress parasitic modes and radiation losses. The via pads and gaps were optimized to match the line impedance to 50 Ω over a broadband frequency response up to 100 GHz. The proposed design consists of a single via transition connecting the signal lines printed on both sides of the LCP layer. The ground vias connect the top and bottom ground layers as well. The effect of the vias is shown in Figure 2B. It shows that a tapered ground of a certain angle (α) requires suppression of the edge radiation. Figure 2B also shows the step-by-step design process adopted to design the optimal results for the transition. The number of vias should be minimized to maintain low manufacturing costs. As illustrated in Figure 2B, four vias should be placed around the signal line for better signal transition (better matching). Another four vias at the edge of the tapered ground plane suppress the radiation (open-end effects). This shows that the via stitched tapered ground has suppressed unwanted radiations effectively to approximately −15 dB.

The radius of the via was 75 μm, which is the smallest feature size that can be mechanically drilled and metalized. The angle (α) of the tapered ground plane was 27° (Figure 2A). The tapering angle of the ground plane was chosen based on the reported research effort for an optimized transition between the CPW and the microstrip lines by matching the impedance and field distributions [11, 13]. The pitch of the vias was 620 μm. The vias suppress the possible resonance and fringing fields of a given structure in the desired frequency band by introducing additional current paths, resulting in low transition loss.

Figure 3 shows pictures of the fabricated prototypes. The fabricated design was fixed by a thick FR4 frame to hold the prototype tightly during the measurement. Figure 4 shows the simulated and measured *S*-parameter results with good agreement. The insertion loss (IL) of the entire structure (back-to-back configuration) for a total length of 6.6 mm was 0.9 dB at 77 GHz. This result corresponds to an IL of 0.45 dB per transition at

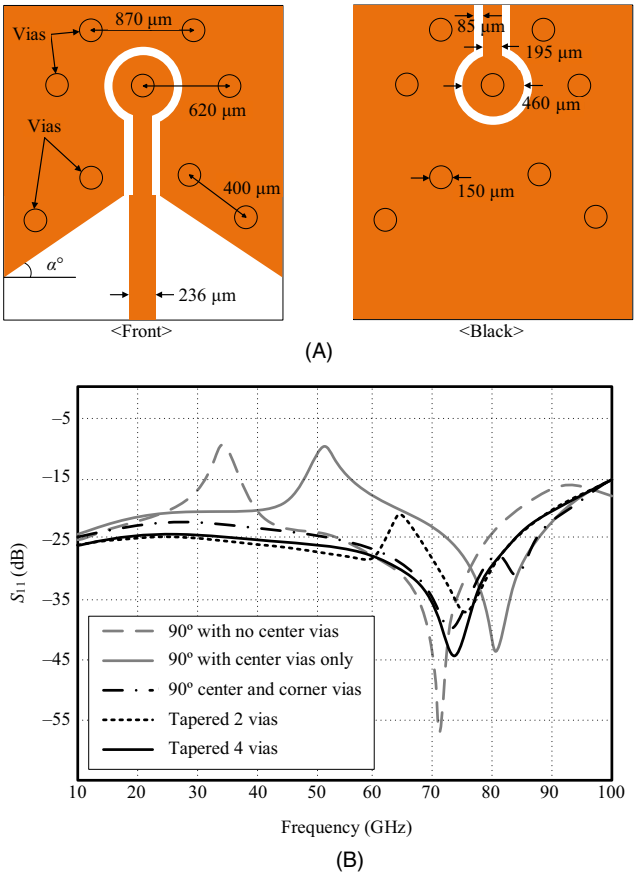

FIGURE 2 (A) Schematic for wideband vertical CPW-CPW-MSTRIP transition and (B) its frequency responses

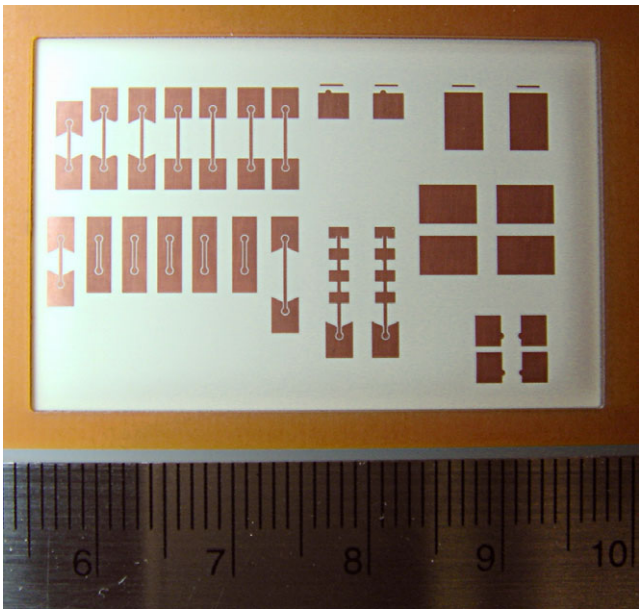

FIGURE 3 Fabricated 3D transitions on LCP with FR4 ring on boundary for mechanical support during measurements

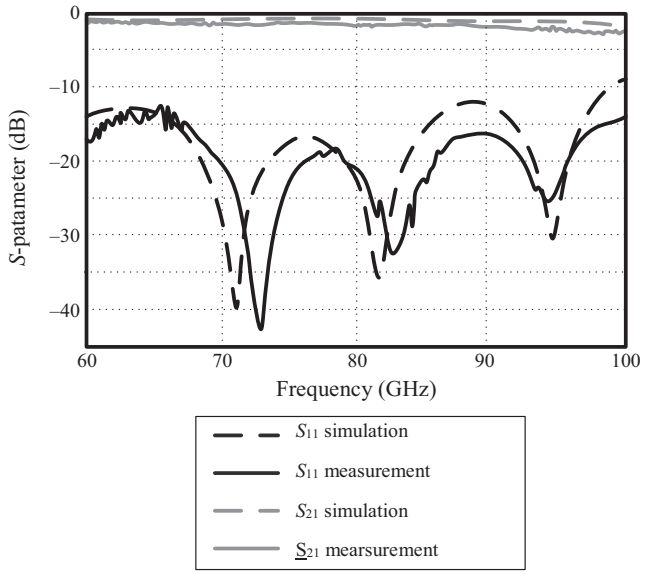

FIGURE 4 *S*-parameters of CPW-CPW-MSTRIP transition

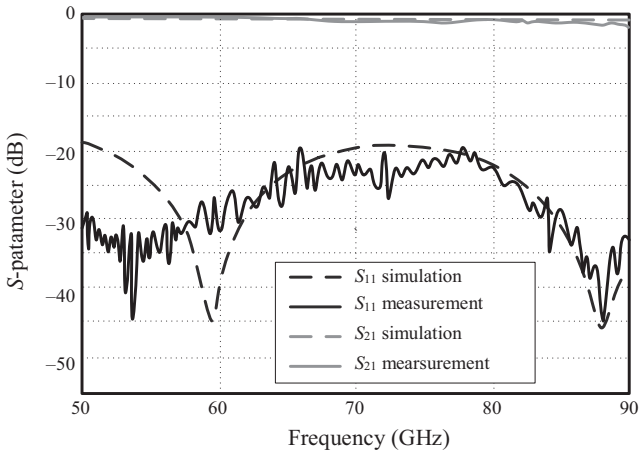

FIGURE 5 *S*-parameters of fabricated 3D CPW-CPW transition

77 GHz and 1.18 dB at 100 GHz. It should be noted that the IL per transition is less than 0.5 dB at 60 GHz to 80 GHz, and 1.2 dB in the frequency range of 80-100 GHz.

2.2 | Coplanar waveguide transitions

A similar design approach was taken for the wideband 3D CPW-CPW transition design. This structure was chosen to investigate the importance of optimal via spacing for the broadband ground plane of the CPW lines. It is important to minimize the use of vias to achieve optimal performance while minimizing cost. Prototypes were fabricated with via spacings of 250, 500, and 1,000 μm to investigate the effect of via spacing. It was found that maintaining a via spacing of 500 μm yielded optimum results that satisfy both the performance and optimal number of vias. The measured *S*-parameters were in good agreement with the simulation results, and the reflection coefficient (S_{11}) values were lower than −20 dB in the 50 GHz to 90 GHz frequency range, as shown in Figure 5.

The measured IL at 77 GHz was 0.5 dB for the back-to-back configuration of the 5.6-mm long transition. This is equivalent to an IL of 0.25 dB for a 2.8-mm long single transition. The optimal number of vias and via-to-via pitch selection of the CPW line are the most important design parameters. It is important to maintain a 600-μm spacing ($\lambda g/4$) of via-via pitch at the center frequency (77 GHz) to suppress unwanted radiation due to the parallel-plate CPW mode.

2.3 | 3D transitions and antenna array integration

The integrated 3D transitions presented in the previous section are useful techniques for broadband parasitic radiation/crosstalk reduction between the antenna-feeding networks and the multichannel/multicore RF front-end system. This radiation reduction was achieved by avoiding any undesired geometrical discontinuities such as sharp edges, significantly long feeding lines, or mismatches between the feeding lines and the loads.

As a proof of concept and without loss of generality, an 8 × 2 microstrip antenna array was designed and fabricated at the center frequency of 77 GHz. This frequency band is commonly used for UWB automotive short-range radars. A schematic of the antenna is shown in Figure 6A in terms of the top and bottom views of the structure. The power splitter (or combiner) is shown in Figure 6A,B. The fabricated AUT is also shown in Figure 6B. The width (*W*), length (*L*), and distance (*D*) between the antenna elements (center-to-center) were 1.2 mm, 1.1 mm, and 2.1 mm, respectively. A chamfered microstrip transmission line and curved tapering of the CPW ground near the microstrip-to-CPW transition were utilized to further minimize the radiation loss. It should be noted that a special step had to be taken to evaluate the radiation performance of the antenna array properly. This is because the receiver inside the mmWave antenna chamber could not hold a probe station. Standard waveguide connectors were required to measure the antenna array in the anechoic chamber. A microstrip-to-waveguide transition was built for the purpose of the test. A WR-10 rectangular waveguide was connected to feed the antenna under test (AUT). A waveguide-to-microstrip transition was utilized to feed the designed antenna array. Figures 7 and 8 shows the S_{11} and gain results, respectively. The discrepancy between the measurement and simulation results has no more than a 5% error range. It should be noted that S_{11} covers the design frequency band of 74 GHz to 81 GHz with a center frequency of 77.5 GHz. The measured antenna gain in the H-plane was 12.3 dBi. The ILs of the microstrip-to-waveguide transition and waveguide-to-

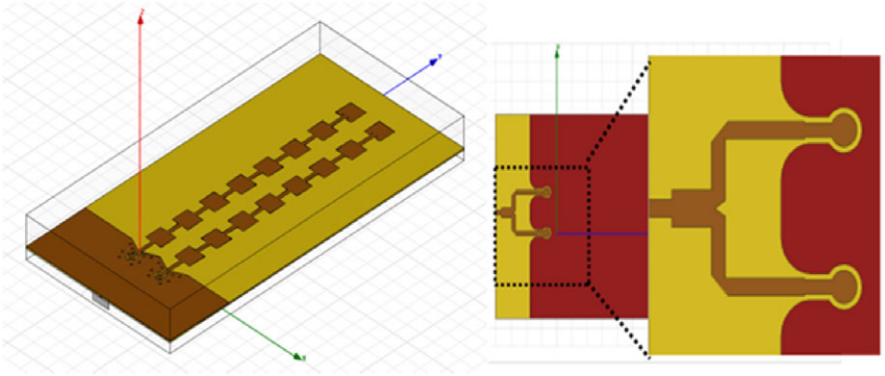

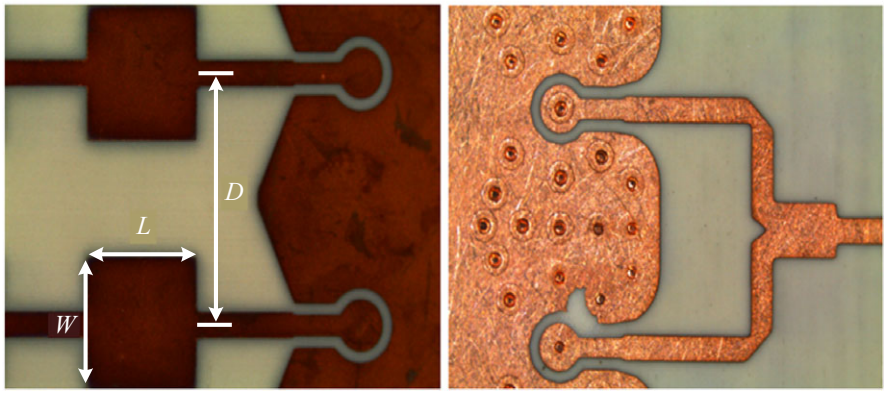

FIGURE 6 (A) Schematic of 8 × 2 prototype array with 3D transition and (B) fabricated AUT

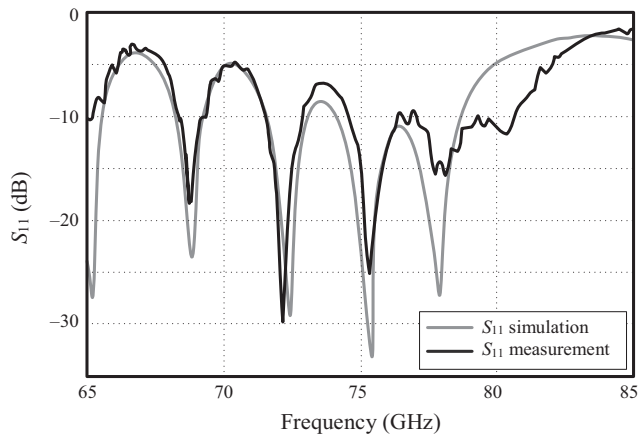

FIGURE 7 Measured S_{11} of 8 × 2 antenna array

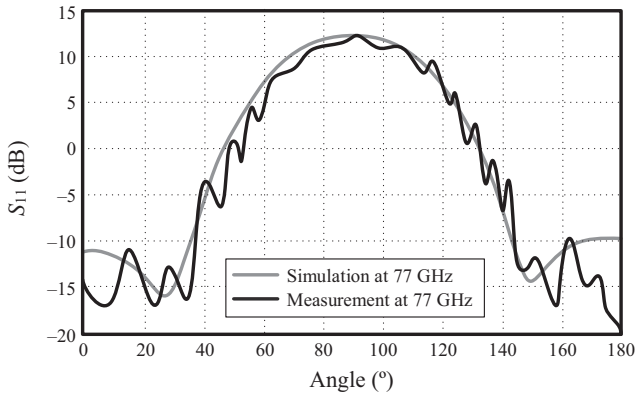

FIGURE 8 Antenna gain of 8 × 2 antenna array

waveguide connection were compensated because they are not part of the antenna system. This section verifies the ideas and concepts of the proposed low-loss broadband 3D transitions for mmWave antenna arrays. The well-designed CPW ground plane acts as an EM shielding, improving isolation, and a heat sink for the TRx module mounted on the backside of the module. This general idea can be expanded to large arrays, such as 8-, 16- and 32-channel configurations.

3 | 16 × 16 ANTENNA ARRAY

This section details the design of a 16 × 16 antenna array that integrates all of the mmWave transitions and interconnection technologies discussed in this paper. The

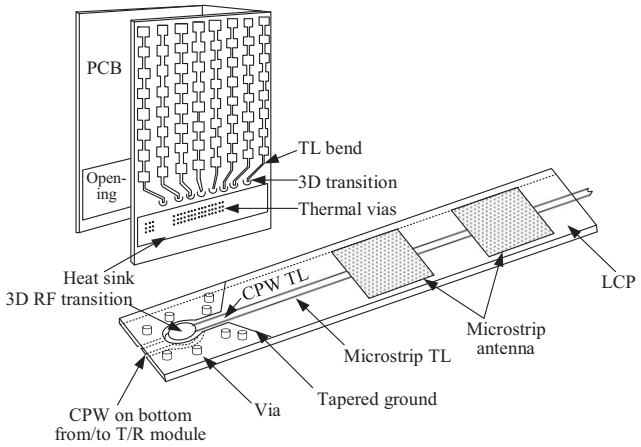

FIGURE 9 Proposed radar front-end assembly: PCB and LCP antenna substrate with 3D RF transition

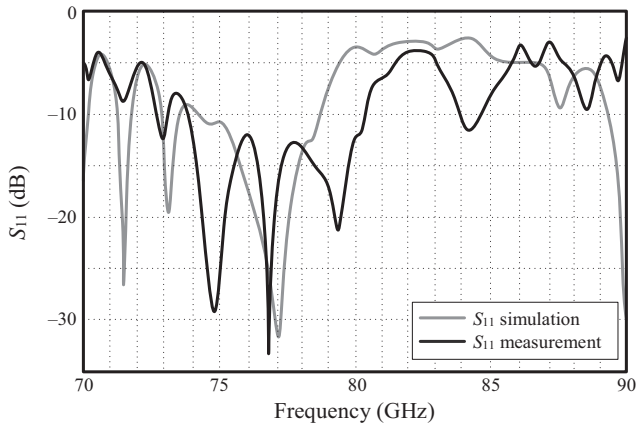

FIGURE 10 Measured and simulated S_{11} of 16 × 16 coupled-fed antenna array

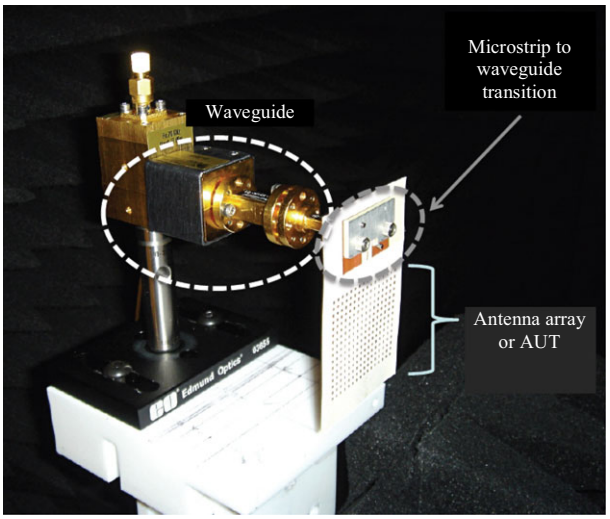

(A)

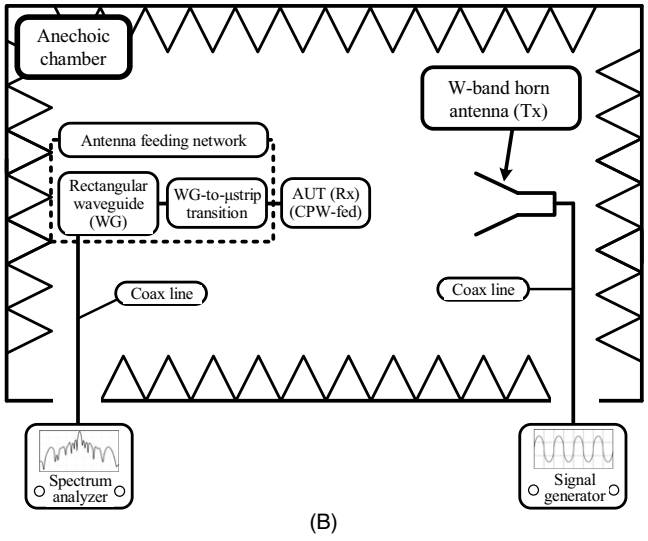

(B)

FIGURE 11 A, Antenna measurement setup and B, block diagram of measurement system

proposed design is shown in Figure 9. Each 16 × 1 individual branch consisted of 16 proximity-coupled patch antennas at a distance of 1 mm. The antennas were fed by an underlying 50 Ω microstrip line that was connected to the TRx module through the CPW-MSTRIP transition, as presented in the previous section. The proposed antenna array utilized two 100-μm thick LCP layers to realize the proximity-coupled patch antenna structure. The microstrip feeding line was sandwiched between the top and bottom layers, and the 16 × 16 antenna array was built on the top layer, as shown in Figure 9. The bottom layer was the ground plane, and it was the reserved space for the TRx IC chips. Each individual microstrip patch element had a length of 1.0 mm and a width of 0.8 mm. The center-to-center separation between the elements was 1.4 mm. The width of the embedded microstrip line was adjusted accordingly to have a 50-Ω impedance looking into the sub-array.

The measured S_{11} of the designed 16 × 16 antenna array is shown in Figure 10. The small discrepancy between the simulation and the measurements can be explained by fabrication error and misalignments. For the S_{11} measurement, an additional microstrip-to-waveguide transition was required to feed the antenna, as depicted in Figure 11 [14]. The total gain in the H-plane of the 16 × 16 antenna array is also shown in Figure 12. The measurements were performed at 77 GHz, and the simulation results correspond well with the measurement results. The peak simulated gain was 23.6 dBi and the measured gain was 21.16 dBi for the H-plane. The proposed antenna has an approximately 5 dBi to 10 dBi higher gain than reported designs [15, 16], and the antenna array with comparable gain presented in [17] has considerably more antenna elements (23 × 29). The performance comparison is summarized in Table 1. The

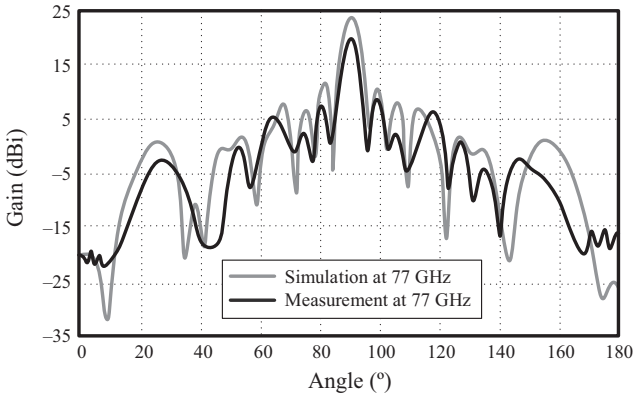

FIGURE 12 Realized antenna gain in H-plane

TABLE 1 Comparison table

	Size (mm)	Design frequency (GHz)	Gain (dBi)
[18]	78 × 77	77	20.0
[19]	50 × 50	77	25.0
This work	38 × 42	77	23.6

antenna-feeding network consisting of a waveguide-to-microstrip transition and a rectangular waveguide (Figure 11B) had a loss of 2.44 dB. The angle of the main lobe shown in Figure 12 varied depending on the operation frequency because the phase of the antenna array elements was not aligned, resulting in a tilted beam with a lower gain. A stable RF source is a critical part of a series-fed array antenna since the antenna array is sensitive to the phase of the input signal.

4 | CONCLUSION

This paper presents the design and integration of a novel 3D-broadband transition and enhanced-gain (more than 20 dBi) antenna array topology on a flexible organic LCP substrate. It is suitable for low-cost, high-performance mmWave modules. The proposed structures are attractive for cost- and size-sensitive applications such as compact automotive radar applications and beam-steering wideband antenna arrays. The presented design also demonstrates the feasibility of a highly integrated, low-cost conformal 3D mmWave RF system-on-package front-end module.

FUNDING INFORMATION

This work was supported by a 2-Year Research Grant of Pusan National University.

REFERENCES

1. World Health Statistics (WHO), *Ten statistical highlights in global public health*, WHO, Geneva, Switzerland, 2007.
2. K. Huang and D. Edwards, *Millimetre wave antennas for gigabit wireless communications*, John Wiley & Sons, Hoboken, NJ, 2008.
3. E. Kasper et al., *High speeds in a single chip*, IEEE Microw. Mag. **10** (2009), no. 7, 28–33.
4. W. Lee, J. Kim, and Y. J. Yoon, *Compact two-layer Rotman lens-fed microstrip antenna array at 24 GHz*, IEEE Trans. Ant. Propag. **59** (2010), no. 2, 460–466.
5. Y.-J. Park and W. Wiesbeck, *Offset cylindrical reflector antenna fed by a parallel-plate luneburg lens for automotive radar applications in millimeter-wave*, IEEE Trans. Ant. Propag. **51** (2003), no. 9, 2481–2483.
6. R. C. Daniels et al., *60 GHz wireless: up close and personal*, IEEE Microw. Mag. **11** (2010), no. 7, 44–50.
7. S. Xiao, M. Zhou, and Y. Zhang, *Millimeter wave technology in wireless PAN, LAN, and MAN*, CRC Press, Boca Raton, FL, 2008.
8. D. Thompson et al., *Characterization of liquid crystal polymer (LCP) material and transmission lines on LCP substrates from 30 to 110 GHz*, IEEE Trans. Micro. Theory Tech. **52** (2004), no. 4, 1343–1352.
9. A. Margomenos, Y. Lee, and L. Katehi, Wideband Si micromachined transitions for RF wafer-scale packages, in *Proc. Topical Meeting Silicon Monolithic Integr. Circuits RF Syst.*, Long beach, CA, Jan. 10–12, 2007, pp. 183–186.
10. A. Stark and A. Jacob, A Broadband vertical transition for millimeterwave applications, in *Proc. Eur. Microw. Conf.*, Amsterdam, Netherlands, Oct. 27–31, 2008, pp. 476–479.
11. Y.-G. Kim, K. W. Kim, and Y.-K. Cho, An ultra-wideband microstrip-to-CPW transition, in *Proc. Int. Microw. Symp. Digest*, Atlanta, GA, June 15–20, 2008, pp. 1079–1082.
12. W. Mayer et al., *Eight-channel 77-GHz front-end module with high-performance synthesized signal generator for FMCW sensor applications*, IEEE Trans. Micro. Theory Tech. **52** (2004), no. 3, 993–1000.
13. G. Zheng, J. Papapolymerou, and M. M. Tentzeris, *Wideband coplanar waveguide RF probe pad to microstrip transitions without via holes*, IEEE Microw. Compon. Lett. **13** (2003), no. 12, 544–546.
14. H.-B. Lee and T. Itoh, *A systematic optimum design of waveguide-to-microstrip transition*, IEEE Trans. Micro. Theory Tech. **45** (1997), no. 5, 803–809.
15. R. Alhalabi and G. Rebeiz, *High-efficiency angled-dipole antennas for millimeter-wave phased array applications*, IEEE Trans. Ant. Propag. **56** (2008), no. 10, 3136–3142.
16. S. Beer, G. Adamiuk, and T. Zwick, *Novel antenna concept for compact millimeter-wave automotive radar sensors*, IEEE Ant. Wireless Propag. Lett. **8**, (2009), 771–774.
17. M. Ettorre, et al., *Single-folded leaky-wave antennas for automotive radars at 77 GHz*, IEEE Ant. Wireless Propag. Lett. **9**, (2010), 859–862.
18. H. Mizuno et al., A forward-looking sensing millimeter-wave radar, in *Proc. JSAE Ann. Congr.*, Japan, 2004, pp. 5–8.
19. T. Binzer, M. Klar, and V. Gross, Development of 77 GHz radar lens antennas for automotive applications based on given requirements, in *Proc. ITG Conf. Antennas*, Munich, Germany, Mar. 28-30, 2007, pp. 205–209.

AUTHOR BIOGRAPHIES

Sangkil Kim received his BSc degree from the School of Electrical and Electronics Engineering, Yonsei University, Seoul, Republic of Korea, in 2010. He received his MSc and PhD degrees from the School of Electrical and Computer Engineering, Georgia Institute of Technology, Atlanta, GA, USA in 2012 and 2014, respectively. From 2015 to 2018, he worked at Qualcomm, Inc., San Diego, CA, USA as a senior engineer. He joined the faculty of the Department of Electronics Engineering, Pusan National University, Busan, Rep. of Korea in 2018. His main research interests are mmWave phased antenna array, RF biosensors, energy harvesting, and printed RF electronics.

Amin Rida received his BSc and MSc degrees in electrical engineering from the Georgia Institute of Technology, Atlanta, GA, USA, in 2006 and 2009, respectively, where he is currently working toward the PhD degree. His research interests include the design, development, and packaging of electronics (antennas, interconnects, 3D transitions, and integration) on organic, flexible, and high-performance substrates for millimeter-wave frequencies. Other research topics focus on X-band filter design and integration in a system on package, characterization of organic substrates for RF applications, antenna design for RFID applications, and the development of wireless transceivers for sensing and power-scavenging applications. He has coauthored a book entitled "RFID-Enabled Sensor Design and Applications" (Boston, MA: Artech House, 2010). Mr. Rida received the IEEE Microwave Theory and Techniques Society (MTT-S) pregraduate scholarship in 2006 and the Best Student Paper Award at the IEEE Antennas and Propagation Symposium, Honolulu, HI, June 2007.

Vasileios Lakafosis received a diploma degree in electrical and computer engineering from the National Technical University, Athens, Greece, in 2006 and an MSc degree in electrical and computer engineering from the Georgia Institute of Technology, Atlanta, GA, USA, in 2009, where he is currently working toward the PhD degree. He has authored and coauthored more than 12 papers in peer-reviewed journals and conference proceedings, and one book chapter. His research interests include networking protocols in the areas of wireless mobile ad hoc, mesh, and sensor networks. Lately, his research has been focused on single- and multihop wireless localization techniques, delay-tolerant and opportunistic networks, and perpetual, low-power network protocols. Mr. Vasileios is a member of the Association for Computing Machinery (ACM) and the Technical Chamber of Greece.

Symeon Nikolaou received a BSc degree in electrical and computer engineering from the National Technical University of Greece (NTUA), Athens, Greece, in 2003, and MSc and PhD degrees from the Georgia Institute of Technology, Atlanta, GA, USA, in 2005 and 2007, respectively. Since September 2007, he has been a lecturer at Frederick University, Nicosia, Cyprus, and an associated researcher at the Frederick Research Center. He has authored or coauthored more than 25 publications in peer-reviewed journals and conferences. His research interests include the design of ultra-wideband (UWB), conformal, and reconfigurable antennas; compact RFIDs; and reconfigurable filters on organic matter.

Manos M. Tentzeris graduated from Ionidios Model School of Piraeus in 1987 and received a diploma degree in electrical engineering and computer science from the National Technical University of Athens (magna cum laude), Athens, Greece, and MSc and PhD degrees in electrical engineering and computer science from the University of Michigan, Ann Arbor, USA, in 1993 and 1998, respectively. He is currently a professor with the School of Electrical and Computer Engineering, Georgia Institute of Technology, Atlanta. He has published more than 370 papers in refereed journals and conference proceedings, 4 books, and 18 book chapters.